Measurement 238 (2024) 115306

Contents lists available at ScienceDirect

Measurement

journal homepage: www.elsevier.com/locate/measurement

Optimizing fracture toughness estimation for rock structures: A soft computing approach with GWO and IWO algorithms

Hadi Fattahi [a], Hossein Ghaedi [a], Danial Jahed Armaghani [b,*]

[a] Faculty of Earth Sciences Engineering, Arak University of Technology, Arak, Iran
[b] School of Civil and Environmental Engineering, University of Technology Sydney, Sydney, NSW 2007, Australia

ARTICLE INFO

Keywords:
Fracture Toughness
Rock Structures
GWO Algorithm
IWO Algorithm
Sensitivity Analysis

ABSTRACT

The importance of mode I fracture toughness (K_{Ic}) lies in its role in studying rock fractures, finding application across diverse sectors like mining, tunneling, and surface construction. Given the time-consuming, costly, and arduous nature of determining fracture toughness through lab and field tests, employing indirect techniques is advised. Soft computing's indirect methods excel at modeling intricate nonlinear connections with optimal efficiency and accuracy, even when geological parameters introduce uncertainty. The innovative aspect of this research lies in leveraging Grey Wolf Optimization (GWO) and Invasive Weed Optimization (IWO) algorithms to model 88 Chevron Notched Brazilian Disc (CCNBD) specimens, designated by ISRM, considering uncertainties. The input parameters encompass uniaxial tensile strength (σ_t), initial crack length (α_0), disc specimen radius (R), crack length (α_B), disc thickness (B), and final crack length (α_1). The research proceeds by employing 80% of the dataset (70 data points) for constructing models via the algorithms, reserving the remaining 20% (18 data points) for model validation. The outcomes, evaluated using statistical metrics such as mean square error (MSE), squared correlation coefficient (R2), mean absolute error (MAE), and root mean square error (RMSE) underscore the exceptional accuracy and performance of GWO and IWO algorithms in predicting and estimating rock structure's K_{Ic}. Moreover, this paper conducts a sensitivity analysis on K_{Ic} estimation's input parameters using @RISK software. Findings reveal that among the input parameters, σ_t exerts the most substantial influence on the model's output. Consequently, even a minor alteration in σ_t yields significant fluctuations in the relationship's output.

1. Introduction

In the context of rock engineering and the stability of structures, the effective control of crack initiation and propagation holds paramount significance. Cracks, whether on a small or large scale, wield notable influence over the strength of rock masses and their deformation [1]. These factors exert a pronounced impact on the stability of various structures, including open mines, underground mines, tunnels, and rock slopes. An equally crucial role is played by rock fracture in the exploration of energy reservoirs, as the generation of fresh cracks contributes to the enhancement and augmentation of oil and gas production [2].

The dynamic and static states of fracture toughness, contingent upon loading conditions relative to the crack, manifest in three distinct failure modes, elucidated in Fig. 1 [3–5].

Illustratively, mode I represents the opening mode, wherein crack displacement occurs perpendicular to the crack front. Mode II embodies the shearing and sliding mode, where crack face displacement transpires along the crack plane but remains perpendicular to the crack front. Lastly, mode III signifies the sliding and tearing mode, characterized by the parallel sliding of the two crack planes along the crack profile line. The International Society of Rock Mechanics has introduced standardized methods, encompassing Mode I and Mode II, for the determination of fracture toughness [6–12], including: SCB (Semi Circular Bend), CB (Chevron Bend), PTS (Punch Through Shear method), SR (Short Rod), SENRBB (Single Edge Notched Round Bar in Bending), CCNBD (Cracked Chevron Notch Brazilian Disc). Throughout the realm of rock mechanics, researchers have persistently explored the expression of rock toughness across various modes, employing diverse direct and indirect methodologies like regression, analytical techniques, and numerical simulations [13–31].

While the insights from the aforementioned approaches are undeniably valuable, their use is limited due to uncertainties related to

* Corresponding author at: School of Civil and Environmental Engineering, University of Technology Sydney, Sydney, NSW 2007, Australia.
E-mail address: danial.jahedarmaghani@uts.edu.au (D.J. Armaghani).

https://doi.org/10.1016/j.measurement.2024.115306
Received 13 April 2024; Received in revised form 24 June 2024; Accepted 11 July 2024
Available online 14 July 2024

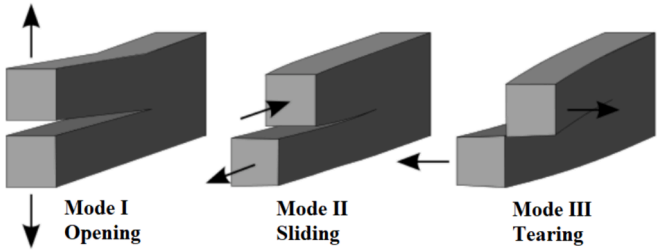

Fig. 1. Various Displacement Modes of Crack Plates [5].

geotechnical parameters. Experimental and analytical methods, despite their advantages, often lack pinpoint accuracy. Their predictions are typically applicable only within specific regions, restricting their extrapolation to other geographical areas. Additionally, numerical methods require the creation of multiple models for each data point because they can only accept single values for geological parameters. Indirect laboratory and field methods, while informative, demand significant time and financial resources due to the need for repetitive experimentation. Furthermore, these procedures, combined with the demands of equipment and the energy expenditure of engineers, may introduce errors in certain cases. Considering these challenges, advancements in technology have led to a compelling alternative: soft computing methods. These methodologies, often implemented through various algorithms within the MATLAB environment, offer a practical solution. Indirect laboratory and field methods, although informative, require considerable time and financial investment due to repetitive experimentation. For instance, the size effect model necessitates multiple specimens of varying sizes to accurately determine fracture parameters, significantly increasing the experimental workload and costs. Similarly, the boundary effect model demands precise control and measurement of boundary conditions, often leading to prolonged experimentation periods and additional financial resources [32,33].

Soft computing techniques effectively address uncertainties and variations in geological parameters while excelling in predicting intricate nonlinear and complex relationships. Notably, these methods are proficient in a cost- and time-effective manner, accounting for the myriad factors that influence model outcomes. By way of illustration, Afrasiabian, Eftekhari [34] harnessed gene expression programming (GEP) and linear multiple regression (LMR) to yield an accurate equation for forecasting mode I fracture toughness (K_{Ic}). Their findings, as evaluated through statistical indices like the R^2 and root mean square error (RMSE), underscored the superior accuracy and performance of gene expression programming. Similarly, Emami Meybodi et al. [35] explored soft computing methods, including support vector regression (SVR), multivariate linear regression (MLR), copula, and multivariate non-linear regression (MNLR), to estimate rock fracture toughness in modes I and II. Their conclusions emphasized the heightened accuracy and functionality of the SVR model in comparison to other methodologies. Roy et al. [34] employed multiple regression techniques alongside soft computational approaches, including the adaptive fuzzy neural inference system, fuzzy inference system (FIS), and artificial neural network (ANN), to simulate crack propagation in rocks resulting from mode-I fracture toughness. The model's outcomes, assessed through statistical metrics such as R^2, MAPE, and RMSE, underscored the superior accuracy of soft computing methods compared to the regression approach. Notably, among the soft computing methods, adaptive neuro fuzzy inference system (ANFIS) yielded the most promising model. Köken and Koca [35], in their pursuit to explore and estimate K_{Ic}, explored diverse methodologies, encompassing ANN, multivariate adaptive regression spline (MARS), ANFIS, and gene expression programming (GEP). Their findings pointed towards the enhanced accuracy of the ANN model. They further suggested that future studies could enhance the model's performance by incorporating additional data. In a parallel study, Dehestani and colleagues [36] employed a machine learning (ML) approach to predict the toughness of travertine, marble, granite, and sandstone across I, II, and combined cone (I-II) modes. To validate their method, three experimental tests were executed. Cao et al. [36] introduced a novel systematic approach utilizing the XGBoost firefly algorithm to predict Young's modulus and unconfined compressive strength of rock. Mohammed [37] employed Vipulandan models to predict mechanical properties, ultimate shear strength of shale rocks, pulse velocity, and fracture toughness. Parsajoo et al. [38] utilized the evolutionary adaptive neural inference system method to estimate the field penetration index of tunnel boring machines in rock masses, demonstrating its high accuracy. Vipulanandan, Mohammed [39] developed a new fracture model, termed Vipulanandan, for sandstone, shale, and limestone, comparing its performance with the Moore-Columbus fracture model based on statistical criteria, root mean square error and coefficient of determination values. Li et al. [40] investigated the impact of stone index tests on predicting the tensile strength of granite samples using fuzzy neural intelligent systems and multiple linear regression methods. Hasanipanah et al. [41] predicted the deformation modulus of rock mass using cascaded feedforward neural networks (CFNN) with algorithms including Bayesian regularization (BR), Lunberg-Marquardt (LMA), and scaled conjugate gradient (SCG), with CFNN-LMA demonstrating superior predictive performance. Jamei et al. [42] forecasted rock brittleness using a robust evolutionary programming model and regression-based feature selection, demonstrating higher accuracy compared to other methods. Fakhri et al. [37], in their investigation, utilized multiple algorithms to assess and quantify the fracture toughness of concrete in central straight notched Brazilian disc (CSNBD) specimens. The resulting model's performance was compared against a range of other algorithms (DT, SVR, KNN, and GPR). Sensitivity analysis of input parameters led to the conclusion that the sample diameter holds greater significance than other parameters. Meanwhile, Mahmoodzadeh and colleagues [38] predicted fracture toughness through the utilization of 12 machine learning models. Their study revealed that gaussian process regression (GPR) and extreme tree regression (ETR) models outperformed other methods in terms of accuracy.

In the context of the aforementioned study, it is pivotal to delve further into the underlying mechanics of the utilized optimization algorithms – the Gray Wolf Optimization (GWO) algorithm and the Invasive Weed Optimization (IWO) algorithm. Optimization algorithms, in general, are computational methods designed to enhance the performance of complex systems by systematically fine-tuning variables or parameters to achieve the best possible outcome. These algorithms simulate the process of evolution or natural behaviors, seeking optimal solutions in diverse problem domainsThe GWO algorithm, drawing inspiration from the social hierarchy and hunting behavior of gray wolves, iteratively updates the positions of wolves to approximate optimal solutions. On the other hand, the IWO algorithm, taking inspiration from the competition and cooperation of invasive plants, mimics the colonization of resources by iteratively updating the population's weed positions to converge towards optimal solutions. The distinct advantage of employing optimization algorithms, such as GWO and IWO, lies in their ability to navigate complex solution spaces, often characterized by multiple variables and intricate relationships, to identify optimal or near-optimal solutions. Traditional analytical methods might struggle to address the nonlinear and multifaceted relationships inherent in estimating fracture toughness. Optimization algorithms, however, excel in capturing these intricate patterns and variations, thereby offering a robust approach to uncertainty quantification and prediction.

Based on the findings of published studies employing soft computing methods, it can be inferred that these approaches offer greater accuracy compared to traditional methods such as analytical, experimental, numerical, and regression techniques. In the current study, the GWO and IWO algorithms are employed as crucial tools for estimating the fracture toughness parameter, KIc, amidst uncertainties. Leveraging the

capabilities of these algorithms aims to present a more precise and efficient alternative to conventional methods, which are often time-consuming, resource-intensive, and constrained in their applicability. The iterative nature of optimization algorithms enables exploration across diverse solution spaces, allowing for adaptive refinement towards optimal outcomes. Thus, the utilization of GWO and IWO facilitates a powerful synergy between computational efficiency and accuracy, facilitating KIc estimation while accommodating the inherent variability and ambiguity in geological parameters. In conclusion, integrating optimization algorithms like GWO and IWO underscores their effectiveness in addressing the challenge of fracture toughness estimation. These algorithms, capable of navigating complex solution landscapes and revealing intricate relationships, represent a promising approach for managing uncertainty in rock mechanics.

To better grasp the primary aim of the aforementioned study, a schematic can elucidate its structure. As depicted step-by-step in Fig. 2, the process begins with the collection of input data necessary for estimating the toughness model of stone structures. In this research, instead of traditional methods, a sophisticated model of high accuracy is developed using the intelligent algorithms GWO and IWO. Subsequently, the model's performance is evaluated using statistical criteria to gauge accuracy and error. Finally, sensitivity analysis is employed to assess the impact of input parameters on the model, providing insights into its robustness and effectiveness.

2. An overview of employed intelligent algorithms

2.1. GWO algorithm

Within the realm of optimizing intricate engineering quandaries, the GWO algorithm, introduced by Mir Jalili et al. in 2014, stands as a novel and pragmatic method [43]. Guided by the social dynamics of actual gray wolves, this algorithm embodies a natural hunting mechanism infused with a structured social hierarchy. This organizational structure employs four distinct wolf roles omega, alpha, delta, and beta to emulate a leadership hierarchy, as depicted in Fig. 3. This hierarchy is orchestrated by a dominant male and female, the alphas, responsible for decision-making and group management, particularly hunting. The beta wolves, positioned in the hierarchy's second tier, assist the alphas and potentially succeed them in leadership roles. Lastly, the omega wolves hold the lowest rank, acting as victims and submitting to their dominant

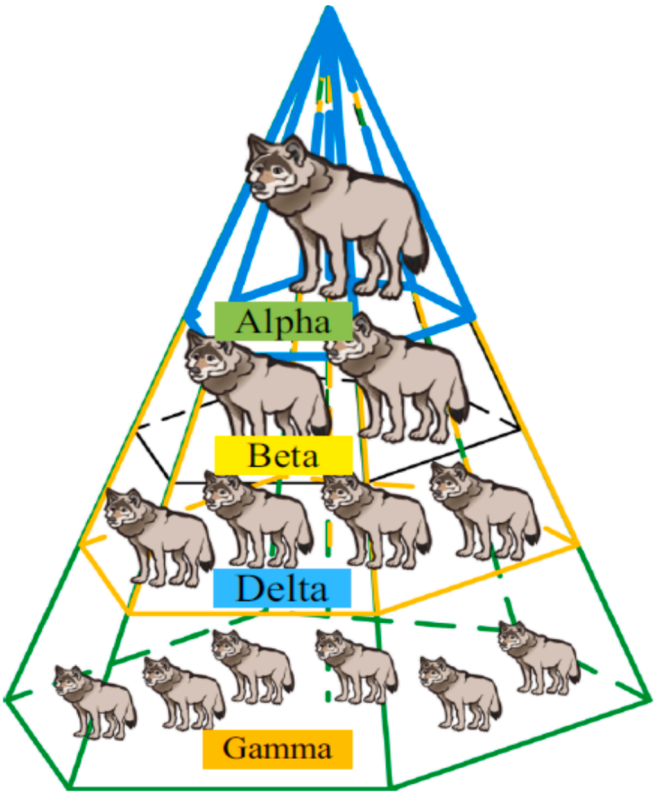

Fig. 3. Hierarchical Structure of Group Hunting of Wolves [43].

counterparts [43].

Significantly, gray wolves display collaborative hunting behavior that aligns with their social structure. This collective effort involves specific stages, including tracking, pursuing, and closing in on prey; surrounding the prey while diverting its path; and ultimately launching an attack on the prey [44,43]:

2.1.1. Mathematical formulation of the algorithm

The GWO algorithm's mathematical underpinnings, essential for problem optimization through coding within the MATLAB environment,

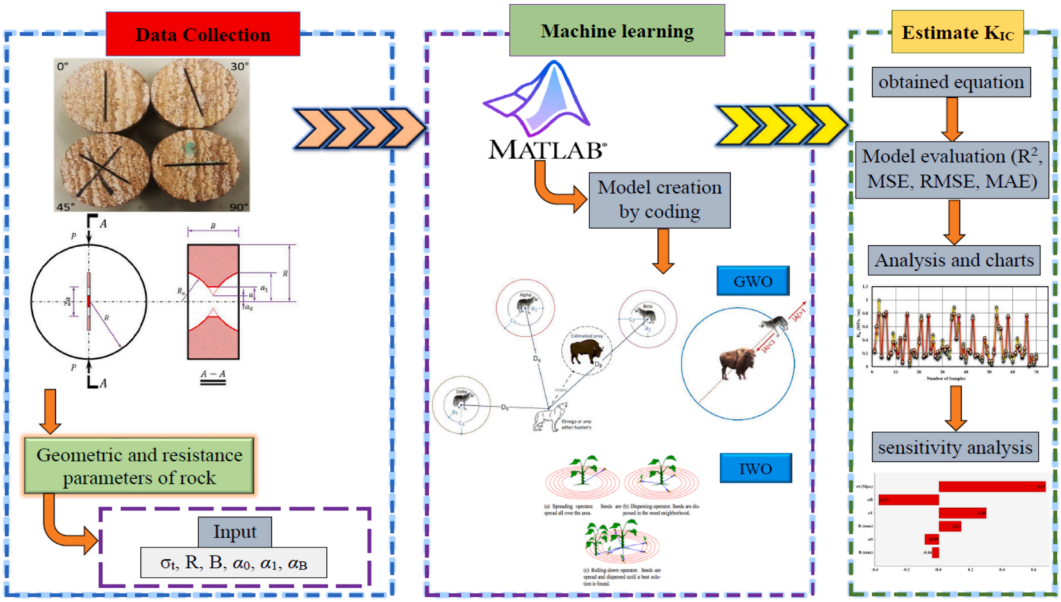

Fig. 2. Schematic of the step-by-step steps in this research.

delve into the hierarchical behavior, encirclement, and attack stages.

2.1.1.1. Social hierarchy. Mathematical representation of the social hierarchy aligns the best solution with the alpha wolf. Following this, the second and third solutions are denoted as beta and delta, whereas all other solutions fall under the omega category. In GWO, the optimization process, akin to hunting, is coordinated by the alpha, beta, and delta wolves, with the omega wolves trailing their lead [43].

2.1.1.2. Modeling the encirclement process. The encirclement behavior, akin to grey wolves' circling of prey during hunting, is mathematically formalized through equations (1) and (2), capturing the dynamics of position vectors and coefficient vectors [43].

$$\vec{D} = \left|\vec{C}.\vec{X}_p(t) - \vec{X}(t)\right| \tag{1}$$

$$\vec{X}(t+1) = \vec{X}_p(t) - \vec{A}.\vec{D} \tag{2}$$

In the above relationships, $\vec{A}$ and $\vec{C}$ coefficient vectors, t is the repetition number, $\vec{X}_P$ hunting position vector and $\vec{X}$ is the position vector of a gray wolf. The vectors $\vec{A}$ and $\vec{C}$ are calculated as follows [43]:

$$\vec{A} = 2\vec{a}.\vec{r}_1 - \vec{a} \tag{3}$$

$$\vec{C} = 2.\vec{r}_2 \tag{4}$$

In this context, the component $\vec{a}$ gradually diminishes across iterations, and random vectors $\vec{r}_1$ and $\vec{r}_2$ contribute to the calculations. Fig. 4 illustrates the positional dynamics of gray wolves during the hunting process.

2.1.1.3. Modeling the hunting process. Grey wolves' hunting behavior is emulated by the top-ranked beta, alpha, and delta wolves, influencing the repositioning of other search agents. Equations (5), (6), and (7) delineate this interplay, steering the movement of wolves toward optimal positioning [43].

$$\vec{D}_\alpha = \left|\vec{C}_1.\vec{X}_\alpha - \vec{X}\right|, \vec{D}_\beta = \left|\vec{C}_2.\vec{X}_\beta - \vec{X}\right|, \vec{D}_\delta = \left|\vec{C}_3.\vec{X}_\delta - \vec{X}\right| \tag{5}$$

$$\vec{X}_1 = \vec{X}_\alpha - \vec{A}_1.(\vec{D}_\alpha),\ \vec{X}_2 = \vec{X}_\beta - \vec{A}_2.(\vec{D}_\beta),\ \vec{X}_3 = \vec{X}_\delta - \vec{A}_3.(\vec{D}_\delta) \tag{6}$$

$$\vec{X}(t+1) = \frac{\vec{X}_1 + \vec{X}_2 + \vec{X}_3}{3} \tag{7}$$

when prey encirclement is complete, the attack phase commences, orchestrated by the alpha wolf. Utilizing vector reduction $\vec{a}$, this process ensures dynamic fluctuation within defined bounds. Fig. 5 depicts the influence of alpha, beta, and delta wolves on the positioning of others.

2.1.1.4. Prey search. For the purpose of determining the positioning of all wolves, the GWO algorithm uses the positions of alpha, beta, and delta wolves as reference points. Figuratively, in state |A|<1, the alpha wolf approaches prey, while in |A|>1, it moves away. This approach facilitates convergence and divergence during the prey search, as illustrated in Fig. 6.

Lastly, Fig. 7 provides an illustrative flowchart capturing the operational trajectory of the GWO algorithm.

2.2. IWO algorithm

The IWO, introduced by Mehrabian, Lucas [45], stands as an intelligent and interactive optimization technique. This algorithm takes inspiration from the reproductive process, survival, and adaptability of

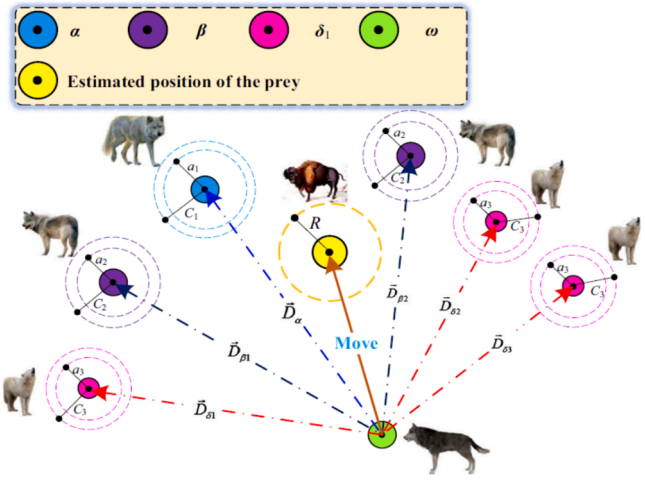

Fig. 5. Impact of Alpha, Beta, and Delta Wolves on Positioning [43].

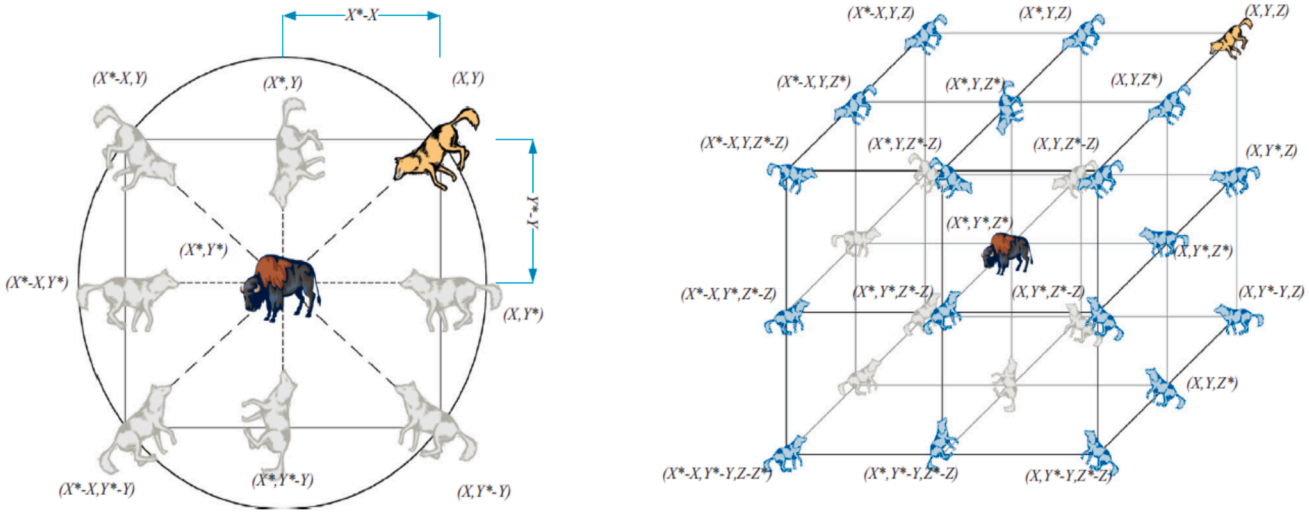

Fig. 4. Two-Dimensional and Three-Dimensional Spatial Vectors during Hunting[43].

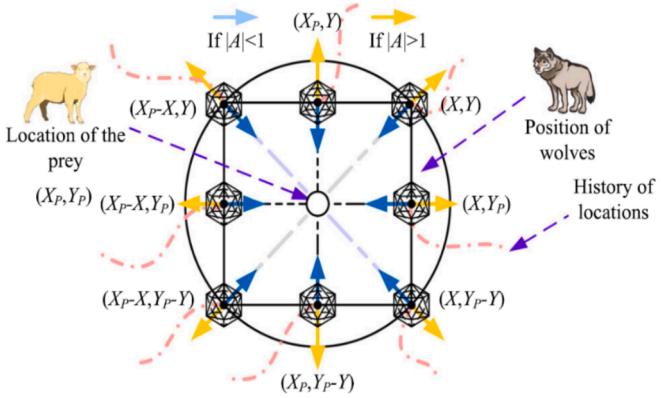

Fig. 6. Convergence and Divergence in Attacking and Searching for Prey [43].

weeds, harnessing their inherent ability to seek optimality, adapt swiftly to environmental conditions, and thrive in changing surroundings. Weeds exhibit a distinct phenomenon wherein they initially produce a multitude of offspring to increase environmental coverage (searching behavior). As capacity becomes constrained, they transition to competitive growth, enhancing quality and adaptability (greedy behavior). In essence, the overarching objective of IWO is to locate the most conducive life environment. The algorithm operates through a series of steps outlined below:

2.2.1. Reproduction

Within this optimization framework, each member of the population generates seeds based on its adaptability. Seed production per plant varies linearly, spanning from a minimal to a maximal seed count. Plants with superior adaptation yield a higher number of seeds. The relationship between adaptation and seed production adheres to equation (8):

$$Seed_n = \frac{f - f_{\min}}{f_{\max} - f_{\min}}(S_{\max} - S_{\min}) + S_{\min} \tag{8}$$

where $Seed_n$ represents seed count, f signifies the current weed's fitness, f_{max} and f_{min} respectively denote the highest and lowest fitness in the population, and S_{max} and S_{min} correspond to the maximum and minimum feasible seed production. Fig. 8 depicts the linear relationship between adaptation and seed production [45].

Based on Fig. 9, it is evident that higher adaptation yields greater seed production.

2.2.2. Spatial dispersion

At this juncture, the generated seeds are dispersed randomly across the multidimensional problem space. Utilizing a normal distribution function, this dispersion ensures that the seeds grow close to their parent plants. The standard deviation (σ) of the normal distribution function gradually decreases from the initial value (σ_{initial}) to the final value (σ_{final}) over the course of iterations. The relationship among standard deviation, iteration count, and nonlinearity index is expressed through equation (9) [45]:

$$\sigma_{iter} = \frac{(iter_{\max} - iter)^n}{(iter_{\max})^n}(\sigma_{initial} - \sigma_{final}) + \sigma_{final} \tag{9}$$

Here, $iter_{max}$ refers to the maximum number of iterations, σ_{iter} signifies the standard deviation value at the iteration stage, and nn is the index of nonlinearity or nonlinear fluctuation. This progressive reduction in standard deviation leads to a nonlinear decrease in the probability of seed dispersion to distant regions, fostering the aggregation of suitable plants and the elimination of unsuitable ones.

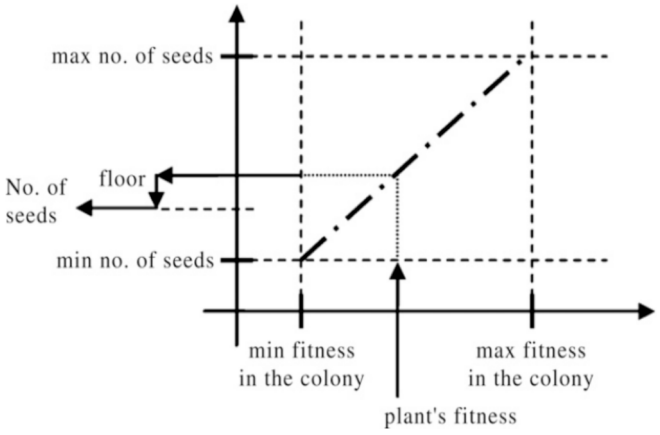

Fig. 8. Seed Production Process in a Weed Colony [45].

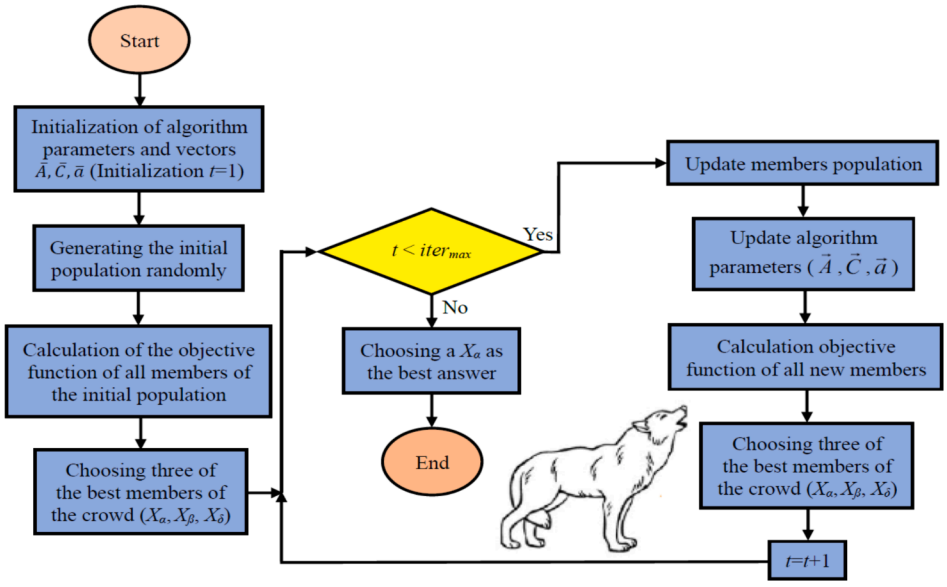

Fig. 7. GWO Algorithm Flowchart[43].

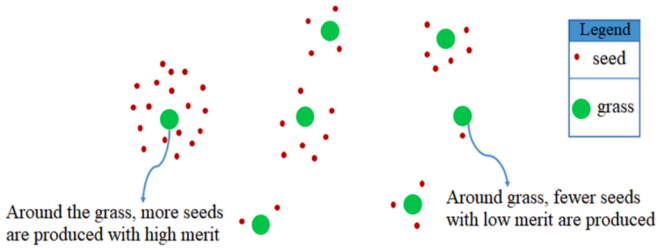

Fig. 9. Graphical representation of algorithm IWO [45].

2.2.3. *Competitive elimination*

As the IWO algorithm progresses through several iterations, the colony's seed count reaches a maximum due to reproduction. To manage this burgeoning seed population and maintain a desirable maximum count (P_{max}), a competitive elimination mechanism is employed. Seeds can continue to generate new ones even after reaching P_{max}, and subsequently, these new seeds disperse across the problem area. Each seed is assigned a score, and in the final step, seeds with lower scores are culled, ensuring the population adheres to the maximum seed count. These actions are iteratively applied until convergence to the ideal configuration is achieved. Fig. 10 illustrates the flowchart depicting the IWO algorithm.

According to the mechanism of GWO and IWO algorithms, the above algorithms and other optimization algorithms can be used to predict material parameters[46–48].

3. Chevron Notched Brazilian disk (CCNBD) for crack analysis

The application of the CCNBD sample, depicted in Fig. 11, was initially introduced by the International Society of Rock Mechanics (ISRM) in 1995 to gauge the fracture toughness of rock specimens. This technique has paved the way for the investigation of fracture mechanisms in Mode I, Mode II, and mixed modes [49,50].

Furthermore, as depicted in Fig. 11, the subsequent relationships can be employed to define dimensionless parameters α_0, α_1, α_B and α_S within the context of ISRM's CCNBD samples:

$$\alpha_0 = \alpha_0/R \tag{10}$$

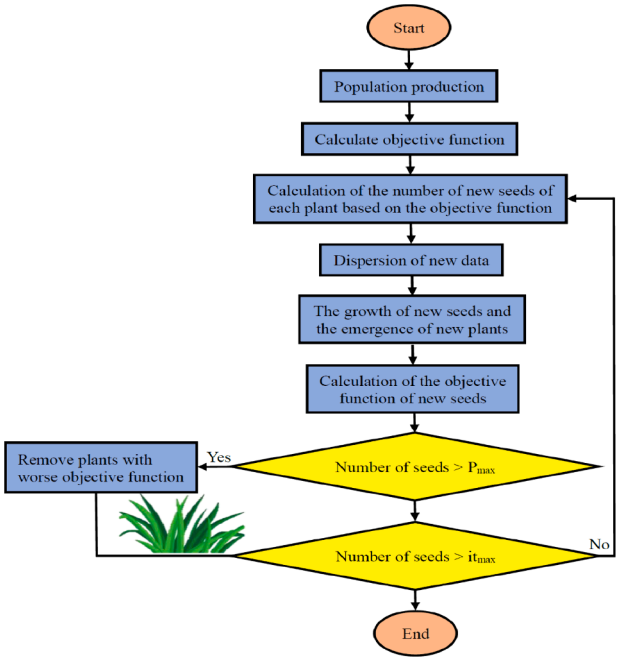

Fig. 10. The flowchart depicting the IWO algorithm [45].

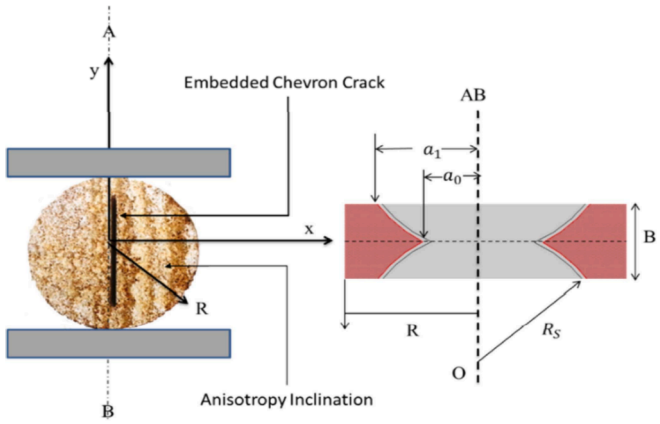

Fig. 11. The geometric properties of CCNBD tests [50].

$$\alpha_1 = \alpha_1/R \tag{11}$$

$$\alpha_B = B/R \tag{12}$$

$$\alpha_S = R_S/R \tag{13}$$

Here, R signifies the radius of the disc specimen, B denotes the thickness of the disc specimen, R_s represents the gap resulting from the chevron saw's two-blade cut, α_0 represents the initial crack length, α_1 signifies the final crack length, α_S indicates the length of the chevron saw gap (created by a two-blade cut), and P represents the applied pressure on the CCNBD sample.

It is worth noting that while the two-dimensional strain mode is commonly used to assess the toughness and fracture behavior of CCNBD samples, its accuracy may vary across different rock geometries. Prior studies have recommended confining the rock sample geometry within the bounds depicted in Fig. 12 to ensure accurate toughness evaluation for various types of rock [51,12].

The subsequent mathematical formulation elaborates on this concept:

$$\alpha_1 \geq 0.4 \quad \text{Line 1} \tag{14}$$

$$\alpha_1 \geq \alpha_B/2 \quad \text{Line 2} \tag{15}$$

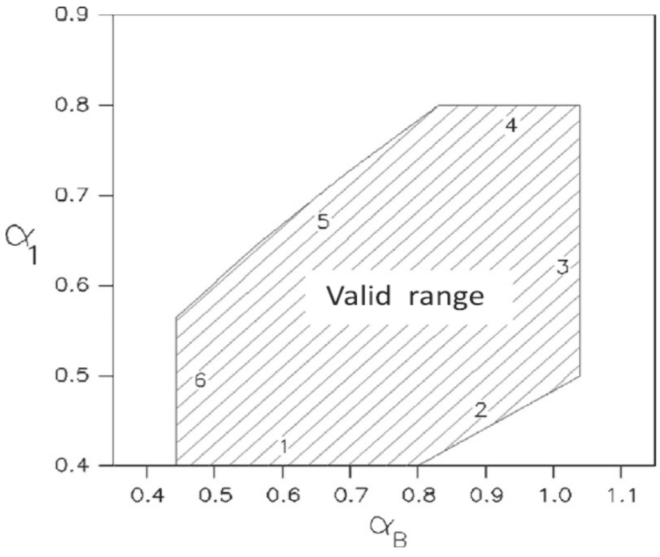

Fig. 12. Outlines the permissible range of values for calculating rock's K_{Ic} in tests recommended by ISRM [50].

$$\alpha_B \leq 1.04 \text{ Line 3} \quad (16)$$

$$\alpha_1 \leq 0.8 \text{ Line 4} \quad (17)$$

$$\alpha_B \geq 1.1729.(\alpha_1)^{5/3} \text{ Line 5} \quad (18)$$

$$\alpha_B \geq 0.44 \text{ Line 6} \quad (19)$$

In scenarios where the fracture process is viewed as linear elastic for CCNBD rock samples, the expression for K_{Ic}, (written as k_I) is as follows [51,52]:

$$k_I = \frac{P_{\max}}{B.\sqrt{R}}.Y^*_{\min} \quad (20)$$

In the aforementioned equation, P_{max} denotes the maximum pressure applied to the CCNBD sample. Additionally, the parameter Y^*_{min} is determined through the following relationship [53,51]:

$$Y^*_{\min} = ue^{v\alpha_1} \quad (21)$$

It's worth noting that the constants u and v in the above relation are established based on the values of α_0 and α_B [54].

4. Input and output data compilation

To establish a robust model using soft computing techniques, a substantial volume of data encompassing both input and output parameters (measurements) obtained from CCNBD test specimens, as recommended by ISRM, is essential. Achieving this necessitated the integration of numerical modeling findings with laboratory experiments conducted in previous studies [54–59]. It's worth noting that, due to the inherent uncertainty in rock parameter properties, researchers and preceding studies have diligently undertaken numerous modeling and laboratory tests to encompass the variability of rock parameter values. Consequently, this study leveraged a dataset comprising 88 data points, amalgamating numerical modeling outcomes (utilizing PFC^{3D} software) and laboratory test results (experimental observations) for CCNBD test specimens as outlined by ISRM.

The considered input parameters within this study encompass uniaxial tensile strength (σ_t in MPa), initial crack length (α_0), radius of the disc specimen (R in mm), crack length (α_B), disc specimen thickness (B in mm), and final crack length (α_1). Furthermore, the prediction and output of the model center around the K_{Ic} of rock structures. For convenience, Table 1 provides a snapshot of the input and output data pertaining to the aforementioned parameters [54–59].

Moving forward, Table 2 furnishes a comprehensive portrayal of statistical information encompassing maximum, minimum, standard deviation, average, and range.

To graphically capture the descriptive statistics of input and output data, a three-dimensional histogram chart coupled with a normal distribution function can be depicted, exemplified in Fig. 13.

To facilitate a more insightful analysis of the input and output data, exploring their correlation proves to be immensely informative. A positive correlation signifies a direct relationship between input and output data, whereas a negative correlation indicates an inverse relationship. A correlation nearing 1 denotes a robust correlation, and conversely, when it approaches 0, the correlation is weak. Understanding the interplay of correlations significantly enhances the modeling process. Within this context, Fig. 14 visually displays the correlation among input and output parameters across the 88 data points. This Figure presents the correlation analysis among the input and output parameters for the 88 data points. The analysis reveals the following key insights:

1. **High Correlation Between Inputs:**
   - o The correlation between the input parameters R (radius) and B (thickness) is notably high at 0.87, indicating a strong positive relationship.
   - o Conversely, the correlation between B and σ_t (tensile strength) is the lowest among input parameters at 0.09, suggesting a weak relationship.
2. **Correlation Between Inputs and Output:**
   - o The parameter σ_t shows a relatively high correlation with K_{Ic} (fracture toughness) at 0.61, highlighting its significant impact on the output.
   - o On the other hand, the parameter R exhibits a low correlation with K_{Ic} at 0.08, indicating a minor influence.

These correlations underscore the varying degrees of influence different parameters have on fracture toughness, which is critical for refining predictive models using GWO and IWO algorithms.

In a broader context, the array of input parameters sets the stage for elucidating the principal objective of this study through a progressive narrative. The crux of this research lies in its assertion that the accurate prediction and assessment of rock structure's K_{Ic} can be realized through the utilization of two algorithms, namely GWO and IWO. To depict this endeavor holistically, Fig. 15 outlines the overarching architecture of the modeling process.

5. Prediction of rock structure K_{Ic} using GWO and IWO algorithms

As previously mentioned, the inherent disparities in rock parameter properties and values at distinct locations make the use of direct techniques like laboratory or field tests laborious, time-consuming, and expensive due to the requisite extensive testing at each point. Moreover, these methods necessitate specialized laboratory equipment and facilities, intensifying the complexity of the work. To mitigate these challenges, alternative approaches such as regression, numerical, experimental, and analytical methods have been employed. However, the intricate and uncertain nature of rock engineering issues often renders the application of these indirect methods imprecise. In light of these limitations, this study employs the GWO and IWO algorithms, developed methods, to forecast and assess the K_{Ic} of rock structures.

With reference to the database section, 88 data points were utilized for this modeling endeavor. Model construction and validation entail the random partitioning of input and output data into two subsets: training and testing. During the training phase, 80 % of the data (70 data points) is utilized to create the relationship using the GWO and IWO algorithms. The remaining 20 % (18 data points) is reserved for model evaluation and verification.

In data-driven modeling techniques, preprocessing of raw data (train and test data) typically involves normalization between 0 and 1 to eliminate outliers and ensure suitability for modeling. The normalization process is executed using Equation (22), resulting in data within the range of 0 to 1. In this equation, X_n signifies normalized data values, X_{mea} denotes actual raw data values, X_{max} represents the maximum data, and

Table 1
A Subset of Inputs and Output Data [50].

No.	Inputs						Output
	σ_t (MPa)	α_0	R (mm)	α_B	B (mm)	α_1	K_{Ic} (MPa.$\sqrt{m}$)
1	13.2	0.297	24.9	0.794	19.76	0.723	1.4
2	13.2	0.321	24.9	0.788	19.62	0.727	1.63
3	13.2	0.273	24.9	0.795	19.8	0.719	1.44
4	13.2	0.249	24.9	0.788	19.62	0.715	1.69
5	13.2	0.361	24.9	0.795	19.8	0.735	1.47
6	13.2	0.289	24.9	0.806	20.06	0.727	1.71
7	13.2	0.333	50.1	0.798	40	0.725	1.73
8	13.2	0.253	50.1	0.798	40	0.715	1.59
9	13.2	0.253	50.1	0.798	40	0.715	1.72
10	13.2	0.222	50.1	0.798	40	0.709	1.71

Table 2
Comprehensive Statistical Description of Inputs and Output Data.

Type	Parameters	Minimum	Maximum	Mean	Range	Std. Deviation
Inputs	σ_t (MPa)	4.60	16.10	10.3511	11.5	5.11345
	α_0	0.211	0.393	0.2693	0.18	0.03324
	R (mm)	24.90	75.25	42.1088	50.35	13.08190
	α_B	0.545	0.8575	0.7201	0.31	0.09959
	B (mm)	17.88	60	29.9609	42.12	9.73261
	α_1	0.604	0.742	0.6792	0.14	0.04369
Output	K_{Ic} (MPa.$\sqrt{m}$)	0.4905	3.325	1.4734	2.83	0.71771

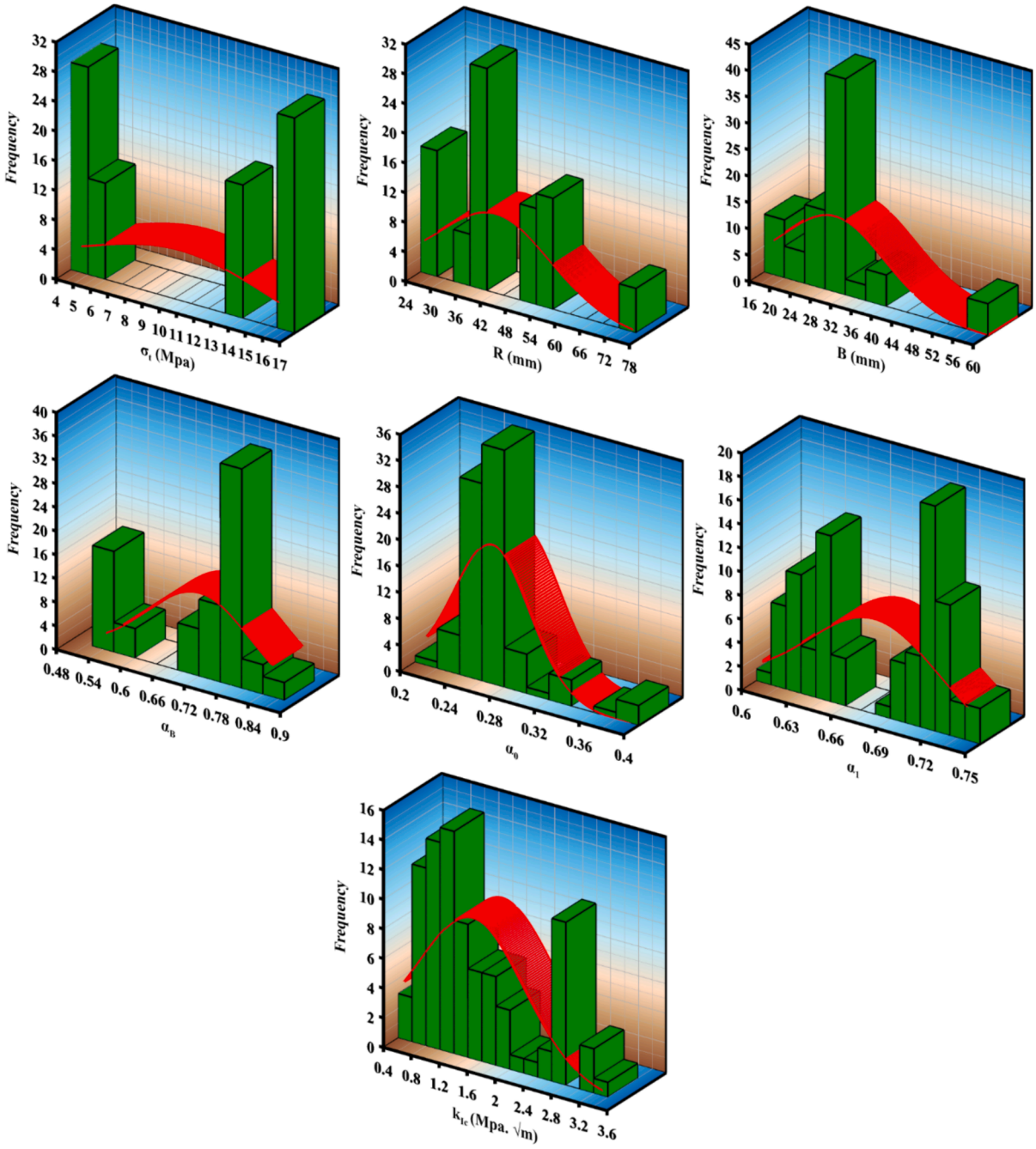

Fig. 13. Histogram Chart Depicting Data Distribution.

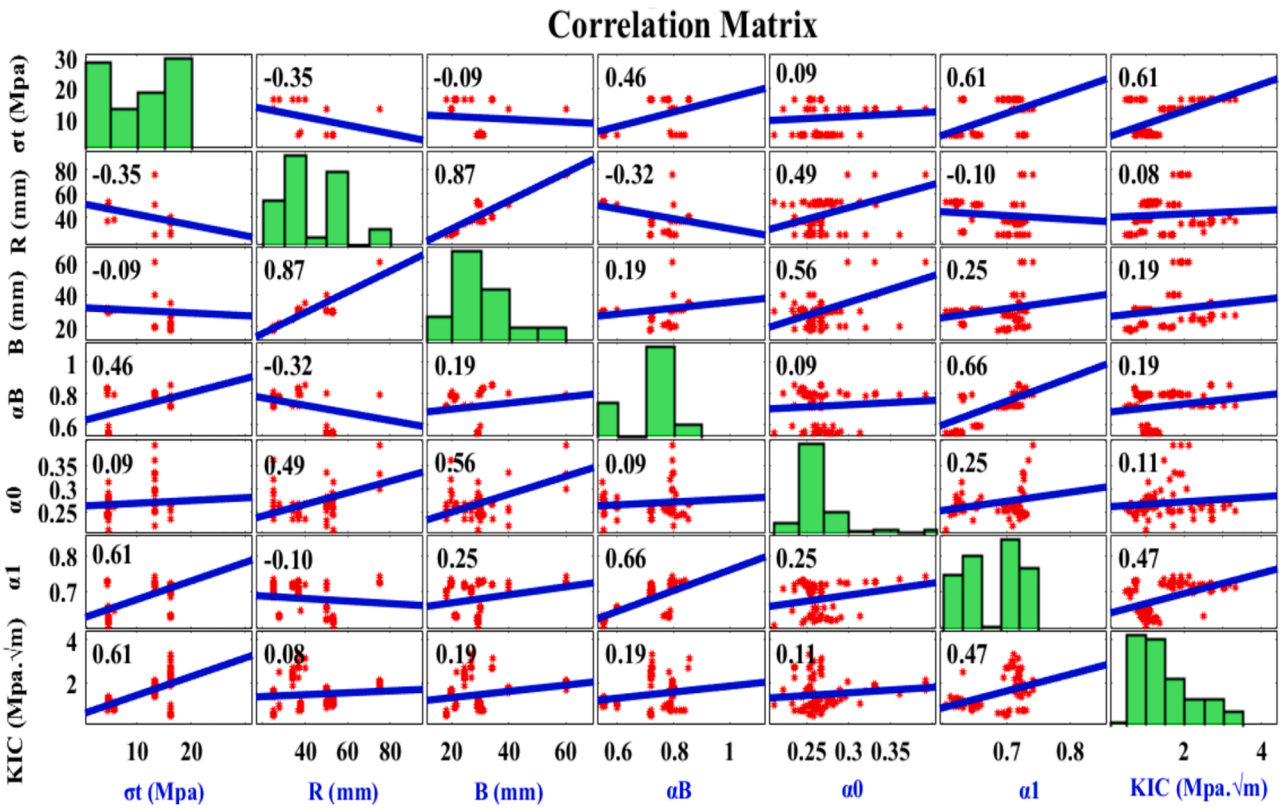

Fig. 14. Visualizing Correlation between Input and Output Data.

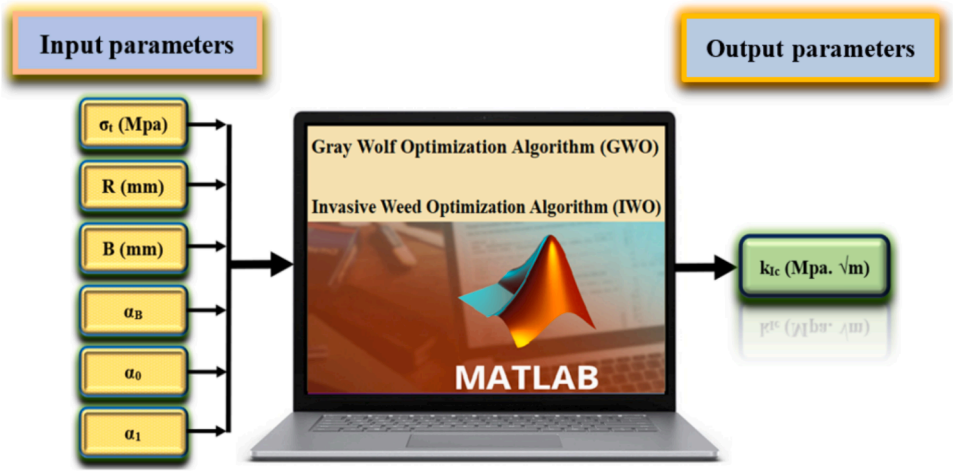

Fig. 15. Visual Representation of the General Modeling Architecture.

X_{min} signifies the minimum data.

$$X_n = [(X_{mea} - X_{\min})/(X_{\max} - X_{\min})] \tag{22}$$

Upon normalizing the training and test data, the estimation of rock structure K_{Ic} through GWO and IWO optimization algorithms necessitates the derivation of two identical nonlinear equations using MATLAB software:

$$k_{Ic}(Mpa.\sqrt{m}) = w_1\sigma_t(Mpa)^{w_2} \times \exp(w_3 R(mm)^{w_4}) - \exp(w_5 B(mm)^{w_6}) - (w_7\exp(\alpha_B^{w_8}))/2 - (\exp(w_9\alpha_0)^2)/2 - w_{10}\exp(\alpha_3^{w_{11}}) - w_{12} \tag{23}$$

Where w_i are weighting variables attributed to input parameters, estimated by GWO and IWO algorithms. Equation (23) was established through trial and error as the optimal means of estimating the K_{Ic} of rock structures. This relationship embodies the most appropriate model for the data, demonstrating minimal error and maximal accuracy. To quantify the performance of the constructed relationship (model), the performance function is defined as:

$$F(v) = \sum_{i=1}^{m} (Y_{mea} - Y_{pre})^2 \tag{24}$$

Here, Y_{mea} and Y_{pre} represent actual and estimated K_{Ic} values of rock structures, respectively, and mm stands for the number of observations.

It is noteworthy that achieving a highly accurate relationship with minimal error for K_{Ic} estimation involves fine-tuning adjustment

Table 3
The values of the setting parameters of GWO and IWO algorithms.

Algorithm	Parameters	Value
GWO	Maximum iterations	3500
	Population number	100
IWO	Maximum iterations	3000
	Variance reduction exponent	8
	Initial value of standard deviation	1.5
	Final value of standard deviation	0.05
	Initial population size	15
	Minimum number of seeds	0
	Maximum population size	100
	maximum number of seeds	25

parameters. These parameters are user-adjusted through iterative trial and error in both GWO and IWO algorithms. The specific tuning parameter values for both algorithms are presented in Table 3.

After establishing the relationship and configuring parameters, prediction coefficients for relationship 8 (to estimate K_{Ic} of rock structures) are obtained for both GWO and IWO algorithms using MATLAB software:

$$k_{Ic}(Mpa.\sqrt{m}) = 2.3185\sigma_t(Mpa)^{5.2911} \times \exp(-0.4138R(mm)^{-0.7515}) - \exp(-1.5953B(mm)^{-6.9052}) - (0.354\exp(\alpha_B^{9.6357}))/2 - (\exp(-0.3424\alpha_0)^2)/2 - (-0.0807\exp(\alpha_3^{5.5595})) - 0.6872 \quad (25)$$

$$k_{Ic}(Mpa.\sqrt{m}) = 6.8092\sigma_t(Mpa)^{6.9286} \times \exp(-1.186R(mm)^{-0.4563}) - \exp(-5.8037B(mm)^{-0.7251}) - (-0.3911\exp(\alpha_B^{9.5657}))/2 - (\exp(-0.1127\alpha_0)^2)/2 - (-0.062\exp(\alpha_3^{7.1629})) - 7.1629 \quad (26)$$

6. Models verification and validation

The assessment and substantiation of the relationships yielded by the GWO and IWO algorithms involved the utilization of key statistical indicators, namely R^2, MSE, RMSE and MAE. In the context of Equations (27) to (29), these metrics are defined with Y_{mea} representing actual values, Y_{pre} representing predicted values, and n signifying the number of data points.

$$R^2 = 1 - \frac{\sum_{k=1}^{n}(Y_{mea} - Y_{pre})^2}{\sum_{k=1}^{n} Y_{mea}^2 - \frac{\sum_{i=1}^{n} Y_{pre}^2}{n}} \quad (27)$$

$$MSE = \frac{1}{n}\sum_{i=1}^{n}(Y_{mea} - Y_{pre})^2 \quad (28)$$

$$RMSE = \sqrt{\frac{1}{n}\sum_{i=1}^{n}(Y_{mea} - Y_{pre})^2} \quad (29)$$

$$MAE = \frac{1}{n}\sum_{i=1}^{n}|Y_{mea} - Y_{pre}|$$

Table 4
Validation of Prediction Models Utilizing GWO and IWO Optimization Algorithms.

Algorithm	Description	R^2	MSE	RMSE	MAE
GWO	Training	0.9267	0.00471	0.06867	0.001731
	Testing	0.9767	0.00224	0.04734	0.00705
IWO	Training	0.9175	0.00532	0.07298	0.00701
	Testing	0.9712	0.00230	0.04800	0.004816

In this context, the proximity of MSE, RMSE and MAE values to zero and the approach of the R^2 value to 1 reflect the precision of the predictive model [60–67]. A model exhibiting such characteristics is deemed an optimal and close-to-reality representation. The computed values of R^2, MSE, RMSE and MAE for the constructed models, facilitated by the GWO and IWO algorithms, were obtained during the training and testing phases, as documented in Table 4.

The discernible insight from Table 4 underscores the notably accurate nature of the K_{Ic} prediction achieved through the GWO and IWO algorithms, with minimal error. To elucidate this point more effectively, Figs. 16 and 17 offer a visual comparison between actual and algorithm-predicted values for both GWO and IWO methods across training and testing phases.

Figs. 16 and 17 distinctly reveal a significant overlap between actual data and the model-predicted values, denoting minimal disparities. This observation implies a close alignment between actual point-to-point values, obtained from field and laboratory tests, and those predicted by the model. As such, the predictive model proves to be a valuable indirect tool for estimating K_{Ic} values of rock structures under analogous geological conditions. This model's applicability extends to other case studies with similar and identical geological settings.

7. Sensitivity analysis

When it comes to gaining a full understanding of how changes in

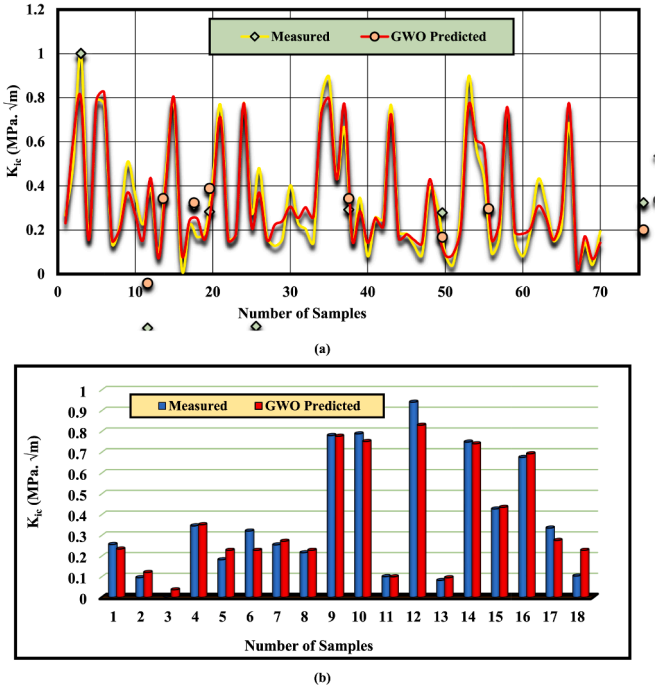

Fig. 16. Comparative analysis of real and GWO-predicted K_{Ic} data: (a) Training phase, (b) Testing phase.

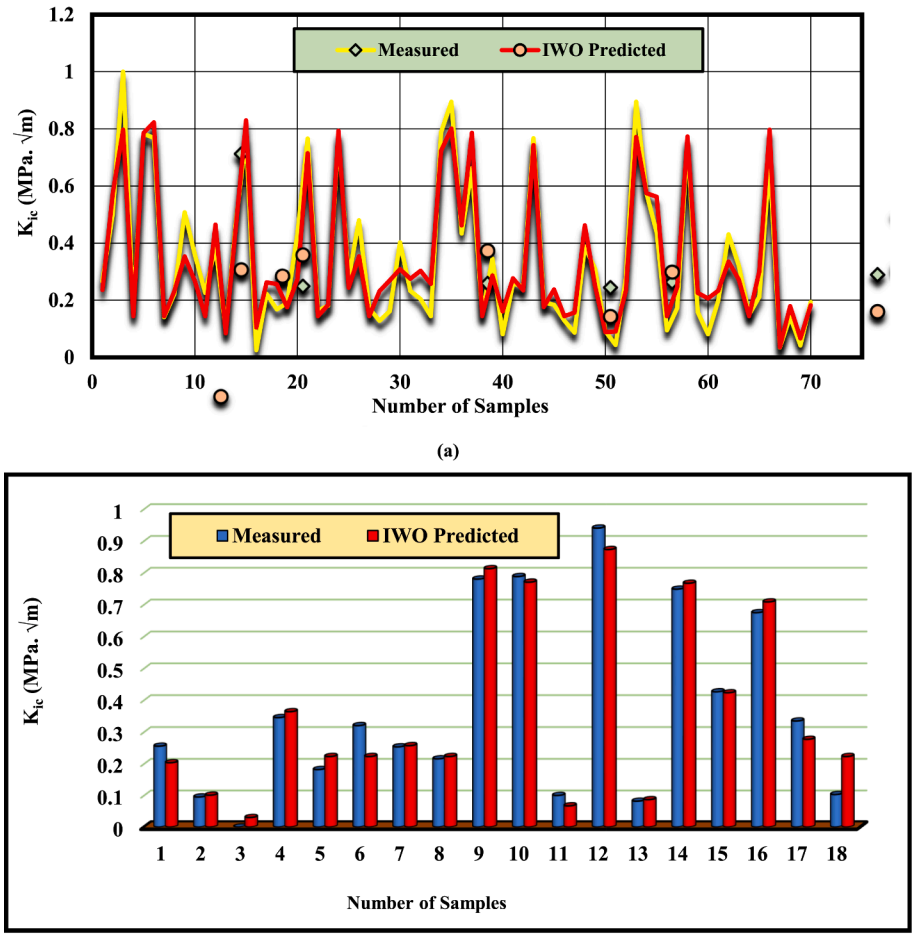

Fig. 17. Comparative analysis of real and IWO-predicted K_{Ic} data: (a) Training phase, (b) Testing phase.

input parameters effect the output of a model or system, sensitivity analysis (SA) is a potent technique that is utilized in a variety of scientific and technical areas. It provides valuable insights into the relative significance of individual variables, shedding light on their contributions to the overall behavior of the system. By systematically varying one or more input parameters while keeping others constant, SA helps reveal which factors have the most pronounced influence and which ones exhibit more subtle effects.

In the context of the K_{Ic} prediction model for rock structures, SA plays a critical role in unraveling the intricacies of the relationships between different input parameters and the resultant K_{Ic} values. This analysis enables researchers and engineers to quantify the degree of responsiveness of the model's output to variations in each input parameter. It also allows the identification of parameters that play a dominant role in shaping the model's outcomes and those that might have a more subdued influence.

Returning to the discussion of our study, SA was meticulously conducted on the K_{Ic} prediction model developed using the GWO and IWO algorithms. The purpose was to delve into the specific effects of the input parameters, namely σ_t, α_0, R, α_B, B, and α_1, on the accuracy of the

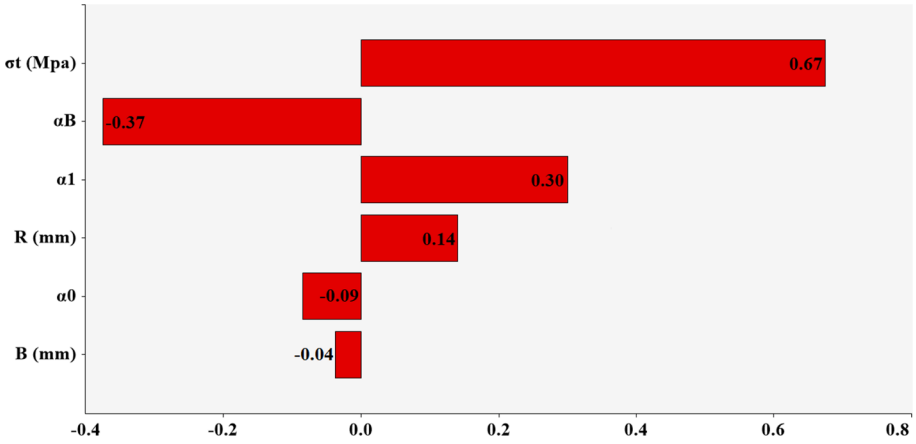

Fig. 18. SA outcomes for the model developed using the GWO algorithm.

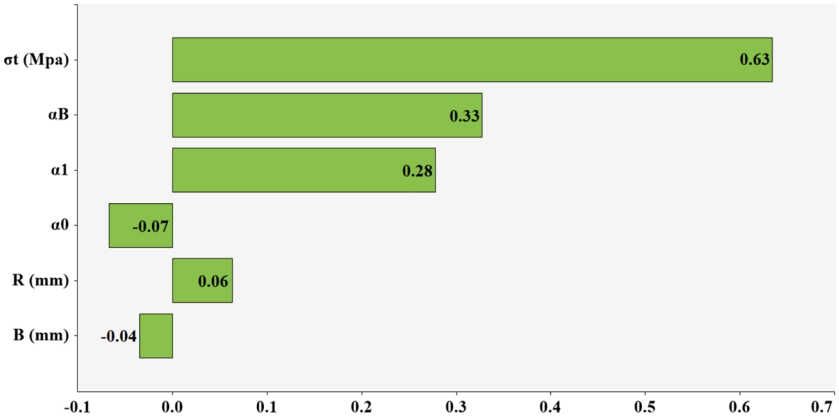

Fig. 19. SA outcomes for the model developed using the IWO algorithm.

predicted K_{Ic} values. By utilizing the @RISK software, the endeavor aimed to unveil the pivotal determinants that wield a prominent influence over the model's outcomes, while also identifying those parameters that exert a more nuanced effect.

The outcomes of this SA are vividly illustrated in Figs. 18 and 19, showcasing the distinct impact of each parameter on the model's predictions for both the GWO and IWO algorithm-based models. Intriguingly, these visual representations highlight the σ_t parameter as a pivotal determinant of the K_{Ic} predictions. The fluctuations and changes in the value of this parameter lead to substantial variations in the predicted K_{Ic} values, underscoring its significance in governing the overall behavior of the model. Fig. 18 provides an insightful view of the SA results for the model developed using the GWO algorithm, while Fig. 19 offers a parallel depiction for the model created with the IWO algorithm. In both cases, the uniaxial compressive strength parameter emerges as a prominent influencer, reinforcing the importance of its accurate determination and emphasizing the need for precise measurements of this parameter in practical applications. According to the results, if the value of the σ_t parameter in equations (25) and (26) changes, even if small, effective changes will occur on the σ_t output. In other words, geotechnical and mining engineers should pay more attention and focus on uniaxial compressive strength. Hence, by leveraging SA, researchers and engineers not only enhance their comprehension of the complex interplay between input parameters and model output but also gain invaluable guidance for refining and optimizing predictive models, ensuring their reliability and effectiveness in real-world scenarios.

8. Research limitations and recommendations for future research

This study primarily focused on predicting the fracture toughness parameter K_{Ic} of rock structures based on appearance parameters, cracks, and uniaxial compressive strength. It is important to acknowledge that additional factors, such as geological and geotechnical rock parameters and other laboratory tests like direct and indirect tensile stress and bending stress, warrant future investigation. In terms of modeling, further research could employ other soft computing methods, including advanced machine learning and intelligent algorithms, to optimize the estimation of fracture toughness for rock structures and compare these methods with the GWO and IWO algorithms. This would allow for a comprehensive evaluation of the suitability of various optimization algorithms for predicting fracture toughness. To enhance the efficiency of soft computing methods, it is advisable for future studies to integrate traditional methods, such as numerical approaches, analytical, and experimental, to compare and validate the results. One limitation of the current method is that the developed relationship is specific to the study area. If the geotechnical and geometric parameters of other case studies are similar or close to those used in this research, the constructed relationship may be applicable. However, if the input parameters differ significantly, a new model must be developed for the new study area. Another limitation is the requirement for proficiency in coding. Engineers and practitioners must be proficient in coding to avoid errors during implementation. If they lack coding skills, these methods may not be recommended due to the high risk of errors.Additionally, soft computing methods require extensive data for effective algorithm training. If the dataset is limited, the efficiency of these methods decreases, and the results may not be reliable.

9. Discussion and conclusions

In the realm of engineering, particularly concerning rock structures, a comprehensive understanding of stability, crack propagation, and failure mechanisms is paramount to mitigating potential risks and financial losses. Accurate prediction and estimation of K_{Ic} are crucial to achieving this objective. The inherent complexities and uncertainties associated with these challenges necessitate sophisticated methodologies capable of encompassing the intricate interplay of various geological parameters. While direct methods (such as laboratory and field tests) and indirect methods (including experimental, analytical, regression, and numerical techniques) are available, the inherent uncertainties in rock parameters demand innovative solutions that transcend conventional practices.

In light of these considerations, this study harnesses the potential of advanced indirect methods, with a particular focus on the GWO and IWO algorithms within the realm of soft computing. Soft computing techniques offer a distinct advantage by harnessing computational power to navigate the complex landscape of geological uncertainties. An inherent benefit of such methodologies is their ability to deliver accurate predictions while optimizing resource utilization. Leveraging these strengths, the research primarily centers on analyzing CCNBD samples, a common choice in laboratory investigations. The study encompasses a comprehensive set of input parameters, including σ_t, α_0, R, α_B, B and α_1. The development of the prediction model involves using a comprehensive dataset comprising 88 data points, subjected to the advanced GWO and IWO algorithms. Within this dataset, 70 data points are dedicated to meticulous model calibration, while the remaining 18 data points serve as a validation set. The validation process, a critical aspect of any predictive model, involves the application of robust statistical metrics, including R^2, MSE, RMSE, and MAE. The outcomes unequivocally affirm the effectiveness of the GWO and IWO algorithms, with the model demonstrating a high degree of alignment between projected and actual values, along with minimal error margins.

Moreover, the study delves into the realm of sensitivity analysis, shedding light on the influence of input parameters in K_{Ic} estimation. Utilizing the @RISK software, the analysis identifies σtσt as the parameter exerting the most substantial influence on the model's

output. This finding underscores the sensitivity of the relationship to variations in σtσt, highlighting its pivotal role in shaping the model's predictions. From the consequences and results of this research, it is evident that since all variable values of input parameters have been investigated in Moore's analysis, measures can be taken to prevent growth and cracking in concrete structures. These methodologies not only alleviate the challenges faced by engineers and craftsmen but also ensure that projects are executed with precision and adherence to timelines. The cost-effectiveness and adaptability of intelligent methods make them an appealing alternative, particularly when tackling intricate and multifaceted rock engineering challenges. These methodologies empower engineers to navigate complex and critical scenarios with unparalleled accuracy and efficacy, transcending the limitations of traditional approaches. The use of advanced optimization algorithms like GWO and IWO enhances the reliability of predictions, minimizes the risk of expensive errors, and ensures the safety and stability of geotechnical projects. Moreover, the limit state function proposed in this study can be adapted to various regions by incorporating local geological and geotechnical conditions, thereby increasing the practical significance of the developed models. Consequently, the research highlights the effectiveness of GWO and IWO in accurately predicting K_{Ic}. These intelligent methods provide substantial improvements in accuracy and efficiency over traditional approaches, offering a dependable tool for K_{Ic} estimation that helps refine design and construction practices in geotechnical engineering.

10. Statement on Ethical Standards

Ethical Approval: This article does not involve studies with human participants or animals conducted by any of the authors.

Informed Consent: All individual participants included in the study provided informed consent.

CRediT authorship contribution statement

Hadi Fattahi: Writing – review & editing, Writing – original draft, Validation, Supervision, Software, Methodology, Investigation, Data curation, Conceptualization. **Hossein Ghaedi:** Formal analysis, Investigation, Methodology, Writing – original draft, Writing – review & editing. **Danial Jahed Armaghani:** Writing – review & editing, Writing – original draft, Supervision, Conceptualization.

Declaration of competing interest

The authors declare that they have no known competing financial interests or personal relationships that could have appeared to influence the work reported in this paper.

Data availability

Data will be made available on request.

References

[1] H. Abe, L. Keer, T. Mura, Growth rate of a penny-shaped crack in hydraulic fracturing of rocks, 2, J. Geophys. Res. 81 (35) (1976) 6292–6298.

[2] T. Funatsu, N. Shimizu, M. Kuruppu, K. Matsui, Evaluation of mode I fracture toughness assisted by the numerical determination of K-resistance, Rock Mech. Rock Eng. 48 (2015) 143–157.

[3] V. Saouma, Fracture mechanics. lecture notes. dept of civil environmental and architectural engineering, University of Colorado, Boulder, USA, 2000.

[4] S. Mohammadi, Extended finite element method: for fracture analysis of structures, John Wiley & Sons, 2008.

[5] M. Ayatollahi, J. Akbardoost, Size and geometry effects on rock fracture toughness: mode I fracture, Rock Mech. Rock Eng. 47 (2014) 677–687.

[6] F. Ouchterlony, Extension of the compliance and stress intensity formulas for the single edge crack round bar in bending, ASTM International. (1981).

[7] Ç. Alkılıçgil, Development of a new method for mode I fracture toughness test on disc type rock specimens, Middle East Technical University, 2006.

[8] L. Tutluoglu, C. Keles, Mode I fracture toughness determination with straight notched disk bending method, Int. J. Rock Mech. Min. Sci. 48 (8) (2011) 1248–1261.

[9] K.P. Chong, M.D. Kuruppu, J.S. Kuszmaul, Fracture toughness determination of layered materials, Eng. Fract. Mech. 28 (1) (1987) 43–54.

[10] M.D. Kuruppu, Y. Obara, M.R. Ayatollahi, K. Chong, T. Funatsu, ISRM-suggested method for determining the mode I static fracture toughness using semi-circular bend specimen, Rock Mech. Rock Eng. 47 (2014) 267–274.

[11] Lim I, Johnston I, Choi S, Boland J Fracture testing of a soft rock with semi-circular specimens under three-point bending. Part 1—mode I. In: International journal of rock mechanics and mining sciences & geomechanics abstracts, 1994. vol 3. Elsevier, pp 185-197.

[12] Fowell R, Xu C The cracked chevron notched Brazilian disc test-geometrical considerations for practical rock fracture toughness measurement. In: International journal of rock mechanics and mining sciences & geomechanics abstracts, 1993. vol 7. Pergamon, pp 821-824.

[13] R. Bearman, The use of the point load test for the rapid estimation of Mode I fracture toughness, Int. J. Rock Mech. Min. Sci. 36 (2) (1999) 257–263.

[14] R.B. Bhagat, Mode I fracture toughness of coal, Int J Min Eng; (united Kingdom) 3 (3) (1985).

[15] T. Backers, O. Stephansson, E. Rybacki, Rock fracture toughness testing in Mode II—punch-through shear test, Int. J. Rock Mech. Min. Sci. 39 (6) (2002) 755–769.

[16] H. Wu, J. Kemeny, S. Wu, Experimental and numerical investigation of the punch-through shear test for mode II fracture toughness determination in rock, Eng. Fract. Mech. 184 (2017) 59–74.

[17] Z. Sun, F. Ouchterlony, Fracture toughness of Stripa granite cores, In: International Journal of Rock Mechanics and Mining Sciences & Geomechanics Abstracts vol 6 (1986) 399–409.

[18] T. Funatsu, M. Seto, H. Shimada, K. Matsui, M. Kuruppu, Combined effects of increasing temperature and confining pressure on the fracture toughness of clay bearing rocks, Int. J. Rock Mech. Min. Sci. 41 (6) (2004) 927–938.

[19] R. Schmidt, C. Huddle, Effect of confining pressure on fracture toughness of Indiana limestone, In: International Journal of Rock Mechanics and Mining Sciences & Geomechanics Abstracts vol 5–6 (1977) 289–293.

[20] J. Bidadi, J. Akbardoost, M.R.M. Aliha, Thickness effect on the mode III fracture resistance and fracture path of rock using ENDB specimens, Fatigue Fract. Eng. Mater. Struct. 43 (2) (2020) 277–291.

[21] J. Guan, Y. Zhang, J. Meng, X. Yao, L. Li, S. He, A simple method for determining independent fracture toughness and tensile strength of rock, Int. J. Min. Sci. Technol. 32 (4) (2022) 707–726.

[22] M. Nejati, A. Aminzadeh, F. Amann, M.O. Saar, T. Driesner, Mode I fracture growth in anisotropic rocks: Theory and experiment, Int. J. Solids Struct. 195 (2020) 74–90.

[23] S.-H. Chang, C.-I. Lee, S. Jeon, Measurement of rock fracture toughness under modes I and II and mixed-mode conditions by using disc-type specimens, Eng. Geol. 66 (1–2) (2002) 79–97.

[24] Q. Xie, X. Liu, S. Li, K. Du, F. Gong, X. Li, Prediction of mode I fracture toughness of shale specimens by different fracture theories considering size effect, Rock Mech. Rock Eng. 55 (11) (2022) 7289–7306.

[25] M. Sistaninia, M. Sistaninia, Theoretical and experimental investigations on the mode II fracture toughness of brittle materials, Int. J. Mech. Sci. 98 (2015) 1–13.

[26] D. Pietras, M. Aliha, T. Sadowski, Mode III fracture toughness testing and numerical modeling for aerated autoclaved concrete using notch cylinder specimen subjected to torsion, Mater. Today:. Proc. 45 (2021) 4326–4329.

[27] O. Oyedokun, J. Schubert, A quick and energy consistent analytical method for predicting hydraulic fracture propagation through heterogeneous layered media and formations with natural fractures: The use of an effective fracture toughness, J. Nat. Gas Sci. Eng. 44 (2017) 351–364.

[28] J. He, L. Liu, W. Yang, M. Aliha, Influence of testing method on mode II fracture toughness (KIIc) of hot mix asphalt mixtures, Fatigue Fract. Eng. Mater. Struct. 45 (10) (2022) 2940–2957.

[29] O. Saeidi, S.R. Torabi, M. Ataei, S. Hoseinie, Prediction of rock fracture toughness modes I and II utilising brittleness indexes, International Journal of Mining and Mineral Engineering 4 (2) (2012) 163–173.

[30] Q. Xie, Y. Zeng, S. Li, X. Liu, K. Du, The influence of friction on the determination of rock fracture toughness, Sci. Rep. 12 (1) (2022) 7332.

[31] S. Zhang, L. Wang, M. Gao, Experimental investigation of the size effect of the mode I static fracture toughness of limestone, Advances in Civil Engineering (2019).

[32] J. Guan, S. Wang, L. Li, C. Xie, M. Khan, L. Niu, Design of rock material parameters by cracked straight through Brazilian disc, Constr. Build. Mater. 402 (2023) 133049.

[33] L. Li, Y. Wang, J. Guan, C. Xie, M. Khan, Normal statistical fracture analysis of Roller-compacted concrete on the basis of non-linear elastic fracture mechanics, Compos. Struct. 324 (2023) 117543.

[34] B. Afrasiabian, M. Eftekhari, Prediction of mode I fracture toughness of rock using linear multiple regression and gene expression programming, J. Rock Mech. Geotech. Eng. 14 (5) (2022) 1421–1432.

[35] E. Emami Meybodi, S.K. Hussain, M. Fatehi Marji, V. Rasouli, Application of machine learning models for predicting rock fracture toughness mode-I and mode-II, Journal of Mining and Environment 13 (2) (2022) 465–480.

[36] J. Cao, J. Gao, H. Nikafshan Rad, A.S. Mohammed, M. Hasanipanah, J. Zhou, A novel systematic and evolved approach based on XGBoost-firefly algorithm to predict Young's modulus and unconfined compressive strength of rock, Eng. Comput. 38 (Suppl 5) (2022) 3829–3845.

[37] A.S. Mohammed, Vipulanandan models to predict the mechanical properties, fracture toughness, pulse velocity and ultimate shear strength of shale rocks, Geotech. Geol. Eng. 37 (2) (2019) 625–638.
[38] M. Parsajoo, A.S. Mohammed, S. Yagiz, D.J. Armaghani, M. Khandelwal, An evolutionary adaptive neuro-fuzzy inference system for estimating field penetration index of tunnel boring machine in rock mass, J. Rock Mech. Geotech. Eng. 13 (6) (2021) 1290–1299.
[39] C. Vipulanandan, A. Mohammed, New Vipulanandan failure model and property correlations for sandstone, shale and limestone rocks, IFCEE 2018 (2018) 365–376.
[40] Y. Li, F.N.S. Hishamuddin, A.S. Mohammed, D.J. Armaghani, D.V. Ulrikh, A. Dehghanbanadaki, A. Azizi, The effects of rock index tests on prediction of tensile strength of granitic samples: a neuro-fuzzy intelligent system, Sustainability 13 (19) (2021) 10541.
[41] M. Hasanipanah, M. Jamei, A.S. Mohammed, M.N. Amar, O. Hocine, K.M. Khedher, Intelligent prediction of rock mass deformation modulus through three optimized cascaded forward neural network models, Earth Sci. Inf. 15 (3) (2022) 1659–1669.
[42] M. Jamei, A.S. Mohammed, I. Ahmadianfar, M.M.S. Sabri, M. Karbasi, M. Hasanipanah, Predicting rock brittleness using a robust evolutionary programming paradigm and regression-based feature selection model, Appl. Sci. 12 (14) (2022) 7101.
[43] S. Mirjalili, S.M. Mirjalili, A. Lewis, Grey wolf optimizer, Adv. Eng. Softw. 69 (2014) 46–61.
[44] C. Muro, R. Escobedo, L. Spector, R. Coppinger, Wolf-pack (Canis lupus) hunting strategies emerge from simple rules in computational simulations, Behav. Process. 88 (3) (2011) 192–197.
[45] A.R. Mehrabian, C. Lucas, A novel numerical optimization algorithm inspired from weed colonization, Eco. Inform. 1 (4) (2006) 355–366.
[46] H. Fattahi, H. Ghaedi, F. Malekmahmoodi, D.J. Armaghani, Optimizing pile bearing capacity prediction: Insights from dynamic testing and smart algorithms in geotechnical engineering, Measurement 230 (2024) 114563.
[47] H. Fattahi, N. Bayat, Developing drilling rate index prediction: A comparative study of RVR-IWO and RVR-SFL models for rock excavation projects, Geomechanics and Engineering 36 (2) (2024) 111.
[48] H. Fattahi, H. Ghaedi, F. Malekmahmoodi, Prediction of rock drillability using gray wolf optimization and teaching–learning-based optimization techniques, Soft. Comput. 28 (1) (2024) 461–476, https://doi.org/10.1007/s00500-023-08233-6.
[49] Ghamgosar M, Erarslan N The effect of cyclic loading amplitude and notch crack inclination angle on the fracture toughness test on Brisbane tuff-multiple factorial analyses. In: ISRM EUROCK, 2014. ISRM, pp ISRM-EUROCK-2014-2046.
[50] Y.-T. Wang, X. Zhang, X.-S. Liu, Machine learning approaches to rock fracture mechanics problems: Mode-I fracture toughness determination, Eng. Fract. Mech. 253 (2021) 107890.
[51] R. Fowell, C. Xu, P. Dowd, An update on the fracture toughness testing methods related to the cracked chevron-notched Brazilian disk (CCNBD) specimen, Pure Appl. Geophys. 163 (2006) 1047–1057.
[52] Y. Xu, F. Dai, T. Zhao, N.-w. Xu, Y. Liu, Fracture toughness determination of cracked chevron notched Brazilian disc rock specimen via Griffith energy criterion incorporating realistic fracture profiles, Rock Mech. Rock Eng. 49 (2016) 3083–3093.
[53] R. Fowell, J. Hudson, C. Xu, X. Zhao, Suggested method for determining mode I fracture toughness using cracked chevron notched Brazilian disc (CCNBD) specimens, International Journal of Rock Mechanics and Mining Sciences and Geomechanics Abstracts 32 (1995) 322A.
[54] M. Aliha, M. Ayatollahi, Rock fracture toughness study using cracked chevron notched Brazilian disc specimen under pure modes I and II loading–A statistical approach, Theor. Appl. Fract. Mech. 69 (2014) 17–25.
[55] M. Aliha, R. Ashtari, M.R. Ayatollahi, Mode I and mode II fracture toughness testing for a coarse grain marble, Appl. Mech. Mater. 5 (2006) 181–188.
[56] Z.-d. Cui, D.-a. Liu, G.-m. An, B. Sun, M. Zhou, F.-q. Cao, A comparison of two ISRM suggested chevron notched specimens for testing mode-I rock fracture toughness, Int. J. Rock Mech. Min. Sci. 47 (5) (2010) 871–876.
[57] M. Wei, F. Dai, N. Xu, T. Zhao, Experimental and numerical investigation of cracked chevron notched Brazilian disc specimen for fracture toughness testing of rock, Fatigue Fract. Eng. Mater. Struct. 41 (1) (2018) 197–211.
[58] M.D. Wei, F. Dai, Y. Liu, N.W. Xu, T. Zhao, An experimental and theoretical comparison of CCNBD and CCNSCB specimens for determining mode I fracture toughness of rocks, Fatigue Fract. Eng. Mater. Struct. 41 (5) (2018) 1002–1018.
[59] M. Aliha, E. Mahdavi, M. Ayatollahi, Statistical analysis of rock fracture toughness data obtained from different chevron notched and straight cracked mode I specimens, Rock Mech. Rock Eng. 51 (2018) 2095–2114.
[60] H. Fattahi, M. Hasanipanah, An indirect measurement of rock tensile strength through optimized relevance vector regression models, a case study, Environ. Earth Sci. 80 (22) (2021) 748, https://doi.org/10.1007/s12665-021-10049-2.
[61] H. Fattahi, M. Hasanipanah, N. Zandy Ilghani, Investigating correlation of physico-mechanical parameters and P-wave velocity of rocks: A comparative intelligent study, J Min Environ 12 (3) (2021) 863–875, https://doi.org/10.22044/jme.2021.11121.2092.
[62] H. Fattahi, Analysis of rock mass boreability in mechanical tunneling using relevance vector regression optimized by dolphin echolocation algorithm, International Journal of Optimization in Civil Engineering 10 (3) (2020) 481–492.
[63] H. Fattahi, A hybrid support vector regression with ant colony optimization algorithm in estimation of safety factor for circular failure slope, International Journal of Optimization in Civil Engineering 6 (1) (2016) 63–75.
[64] H. Fattahi, A new approach for evaluation of seismic slope performance, International Journal of Optimization in Civil Engineering 10 (2) (2020) 261–275.
[65] H. Fattahi, N. Babanouri, Z. Varmaziyari, A Monte Carlo simulation technique for assessment of earthquake-induced displacement of slopes, J Min Environ 9 (4) (2018) 959–966.
[66] H. Fattahi, H. Nazari, A. Molaghab, Hybrid ANFIS with ant colony optimization algorithm for prediction of shear wave velocity from a carbonate reservoir in Iran, Int J Min Geo Eng 50 (2) (2016) 231–238.
[67] H. Fattahi, N. Zandy Ilghani, Hybrid wavelet transform with artificial neural network for forecasting of shear wave velocity from wireline log data: a case study, Environ. Earth Sci. 80 (1) (2021) 5, https://doi.org/10.1007/s12665-020-09320-9.